Biosensors and Bioelectronics 85 (2016) 16–24

Contents lists available at ScienceDirect

Biosensors and Bioelectronics

journal homepage: www.elsevier.com/locate/bios

Sensitivity Enhancement of Bead-based Electrochemical Impedance Spectroscopy (BEIS) biosensor by electric field-focusing in microwells

Kyeong.-Sik. Shin [a], Jae Hoon Ji [a,b], Kyo Seon Hwang [a], Seong Chan Jun [b], Ji Yoon Kang [a,*]

[a] Center for BioMicroSystems, Korea Institute of Science and Technology, Seoul, Korea
[b] Department of Mechanical Engineering, Yonsei Univsersity, Seoul, Korea

ARTICLE INFO

Article history:
Received 21 January 2016
Received in revised form
22 April 2016
Accepted 26 April 2016
Available online 27 April 2016

Keywords:
Magnetic beads
Electrochemical Impedance Spectroscopy (EIS)
Prostate-Specific Antigen (PSA)
Limits of Detection (LOD)

ABSTRACT

This paper reports a novel electrochemical impedance spectroscopy (EIS) biosensors that uses magnetic beads trapped in a microwell array to improve the sensitivity of conventional bead-based EIS (BEIS) biosensors. Unloading the previously measured beads by removing the magnetic bar enables the BEIS sensor to be used repeatedly by reloading it with new beads. Despite its recyclability, the sensitivity of conventional BEIS biosensors is so low that it has not attracted much attentions from the biosensor industry. We significantly improved the sensitivity of the BEIS system by introducing of a microwell array that contains two electrodes (a working electrode and a counter electrode) to concentrate the electric field on the surfaces of the beads. We confirmed that the performance of the BEIS sensor in a microwell array using an immunoassay of prostate specific antigen (PSA) in PBS buffer and human plasma. The experimental results showed that a low concentration of PSA (a few tens or hundreds of fg/mL) were detectable as a ratio of the changes in the impedance of the PBS buffer or in human plasma. Therefore, our BEIS sensor with a microwell array could be a promising platform for low cost, high-performance biosensors for applications that require high sensitivity and recyclability.

1. Introduction

Enzyme-Linked Immunosorbent Assay (ELISA) is a prevalent immunoassay method, and most of the ELISA assays have a detection limit above the range of a few tens of pg/mL (Johnson and Kotowski, 1993). *However, some target biomolecules exist in a sample with very lower concentration range, the ELISA fails to detect these target and cannot report meaningful information. Therefore, it is important to provide a highly-sensitive, reliable, low-cost detection method for early diagnosis and precise monitoring of a disease in blood.* Many researchers have developed various types of biosensors for use as immunoassay devices based on several principles, i.e., electrochemical principles (Akter et al., 2014; Chiriaco et al., 2013; Chuah et al., 2012; Hu et al., 2013; Mao et al., 2012; Zhang et al., 2015), optical principles (Brazhnik et al., 2015; Ewers et al., 2011; Haes et al., 2005; Lee et al., 2015), electrical principles (Choi et al., 2013; Gao et al., 2012; Huang et al., 2013; Luo and Davis, 2013; Oh et al., 2013), and the principles of mechanical transducers (Lee et al., 2005; Wu et al., 2001). Among them, the electrochemical sensors and the nanotechnology(NT)-based field effect transistor (FET) sensors using nanowires (Huang et al., 2013; Kim et al., 2007) or carbon nanotubes (Li et al., 2005) are the most promising for detecting the low concentration range of 10–100 fg/mL (Centi et al., 2007; Gao et al., 2014; Kim et al., 2007; Mohd Azmi et al., 2014). However, it has been difficult to commercialize the NT-based FET sensors due to the long-term instability of their electrical characteristics, which is caused by the diffusions of ions from high ion-strength buffers into gate oxides (Wen et al., 2011).

Electrochemical sensors are advantageous due to their inherent simplicity, low cost of fabrication, and reliability in detecting biomarkers (Rusling, 2013). The electrochemical impedance spectroscopy (EIS) sensors measure changes in the electrical impedance spectrum generated by the interactions between biomarkers and receptors. The region for receptor immobilization is mostly on the surfaces of the electrodes or in the gaps between electrodes, and the changes in the electrical properties that are caused by the interactions between antibodies and antigen can be measured. The direct immobilization of antibodies on the surface of the electrodes hinders the repeated use of EIS sensors and causes problems in their calibration. Hence, a particle-based, renewable, electrochemical immunosensor was proposed that used magnetic beads and gold nanoparticle labeling (Liu and Lin, 2005). The antibody-conjugated magnetic beads were attracted to the surface of a carbon paste sensor by a magnetic field, the beads were washed away from the surface of the sensor for reuse.

* Corresponding author.
E-mail address: jykang@kist.re.kr (J.Y. Kang).

http://dx.doi.org/10.1016/j.bios.2016.04.086
0956-5663/

Several groups also have reported particle-based EIS sensors to detect different target molecules (Centi et al., 2007; Liu and Lin, 2005; Sarkar et al., 2008). However, their LODs (> 100 pg/mL) were so much greater than those of recently reported EIS sensors with signal amplification (5.4 pg/mL) (Yang et al., 2015) or with nanochannels (250 fg/mL) (Nagaraj et al., 2014).

In order to overcome the low sensitivity of conventional particle-based EIS sensors, we propose a new bead-based EIS (BEIS) sensor with high sensitivity as well as reusability. This sensor system is composed of an EIS electrode array with microwells, a magnetic bar to manipulate magnetic beads and a simple straight microfluidic channel to inject the magnetic beads and other reagents. While the magnetic beads of the antibody coating are trapped in the microwells, a sample is injected and the reaction with antigens occurs changes in the impedance of the surfaces of the beads, and makes the difference with the beads incubated in a negative control sample. After the difference is measured, the replacement of the used beads with new beads of the same or a different antibody allows the reuse of the BEIS platform. Sensitivity was enhanced by using a microwell array in which the magnetic beads were located during the measurement of impedance. The microwell improves the sensitivity by concentrating the electric field on the surfaces of the magnetic beads and *also enhances the reliability by maintaining the uniform number of magnetic beads.*

The performance of the BEIS platform with a microwell array was demonstrated by the immunoassay of prostate specific antigen (PSA), which is a protein produced by the prostate gland and which is a sensitive biomarker of prostate cancer or other prostate disorders (Jia-dong et al., 2014; Shariat et al., 2011). *It is well known that the PSA concentration for a normal person ranges from 0 to 4 ng/mL in serum (Jang et al., 2015). Elevations in PSA between 4.0 and 10.0 ng/mL, as compared with PSA levels of less than 4.0 ng/mL, increase the odds of clinically significant (Association, 2000). Although the meaningful clinical level of PSA concentration is very higher than the LODs in most biosensors*, many research groups have conducted the immunoassay of PSA to determine the performance of the biosensors. One of the best LODs was achieved by nano-FET at the level of 1 fg/mL (Kim et al., 2007). We also have tested the performance of BEIS with a microwell array by detecting PSA in Phosphate-buffered saline (PBS) buffer as well as in human plasma, and the LOD of the proposed sensor platform was comparable to that of nano-FET. It will be a promising sensor platform since it can provide a non-labeled, low-cost, reusable sensor that has high sensitivity.

2. Materials and methods

2.1. Regents and preparation of samples

For the preparation of magnetic beads with prostate-specific antigen (PSA) antibody, we purchased tosylactivated magnetic beads (Dynabeads M-280, *diameter* ~2.8 μm) and monoclonal anti-PSA (10-P20A) from Invitrogen and Fitzgerald Industries, USA, respectively. The anti-PSA antibody of *1 mg/mL* was immobilized to the tosylactivated beads in 0.1 M phosphate buffer by incubation for 24 h on a roll mixer in an incubator at 37 °C. The beads were washed with PBST (PBS including 1% Tween 20), and then concentrated to 30 mg/mL in PBST (0.01% Tween 20). The magnetic beads were diluted in 0.1x PBS (mixture with 1x PBS and deionized water) at a concentration of 3 ng/mL. For detection of the PSA antigen (30C-CP1017) that was purchased from Fitzgerald Industries, PSA was prepared with various concentrations, i.e., ranging from 10 fg/mL to 100 pg/mL with 0.1x PBS buffer solution.

2.2. Fabrication and structures of the BEIS platform

The fabrication process for a BEIS sensor is mainly metal patterning on a commercial slide glass (or silicon dioxide wafer) as shown in Fig. S1 in the supplementary. In order to remove any organic contamination on the surface of a starting material, it was cleaned by piranha cleaning process. Then, device patterns including electrodes transferred to a slide glass by image reversal process using AZ5214E by photolithography process. Titanium and platinum was sputtered with the thicknesses of 20 nm and 150 nm, respectively. Then the lift-off process was used to make all of the metal patterns. SU-2005 was used to make the microwells on the metal patterns, and its layer also was used as a passivation of the electrodes. The glass substrate was cured at 180 °C for 30 min on a hotplate. In addition, a microfluidic channel mold was prepared by the conventional lithography method using *SU-8 2005*. A straight line pattern (width: 1 mm, length: 2 cm, depth: 100 μm) was formed on a blank silicon substrate by the SU-8 process. Due to the silicon substrate-Polydimethylsiloxane (PDMS) adhesion problem, we had to treat the surface of the silane on the silicon mold before pouring the PDMS. Then, PDMS was poured onto the silicon substrate and degassed. After curing at 70 °C for 1 h, the PDMS layer was peeled off from the substrate, and the undesirable residues were cut around a straight channel. After making reservoir holes in the PDMS channel, the channel and the detection devices were aligned and bonded, and this was followed by oxygen plasma treatment.

Fig. 1(a) shows the photographs of a fabricated BEIS sensor and a BEIS platform with a PDMS microfluidic channel. A layer of SU-8 was used to construct a microwell on each electrode pair to concentrate the electric field inside the microwell by preventing undesirable leakage current between the metal line and the buffer solution in the microfluidic channel. This platform has multiple microarrays of BEIS sensors with a microfluidic channel on a slide glass or a silicon dioxide substrate, and a permanent magnetic bar beneath a slide glass. *Each BEIS sensor consisted of a 10 × 10 array of a microwell with an electrode pair (the width of working/counter electrode ~ 2 ± 0.2 μm, gap ~ 2 ± 0.2 μm). The individual well diameter and depth were 6 ± 0.5 μm and 5 ± 0.2 μm, respectively. Therefore, each microwell could capture two or three magnetic beads if the diameter of a bead is 2.8 μm.*

2.3. Experimental procedures and electrical measurement for PSA detection

Fig. 1(b) shows the experimental procedure using a BEIS platform. After attaching the anti-PSA antibody onto the magnetic beads, the magnetic beads were injected into the microfluidic channel at a flow rate of 2 μl/min, the beads were attracted into the inside of a microwell array by a magnetic bar located beneath the bottom of a sensor. Then, the residual beads on the SU-8 surface were removed by the injection of PBS buffer solution. After the washing step, a solution of PSA antigen was injected into the microfluidic channel with a flow rate of 2 μl/min, and the flow was stopped for 10 min while the PSA antigen was fully diffused into the bottom of the microwell array and reacted with the antibody on the surface of the beads. After reaction between the anti-PSA antibody and antigen, the PBS buffer was used to remove non-specific binding for a few minutes. The impedance of the BEIS platform was measured after stopping the flow of solution. After finishing a measurement, last two steps were repeated to measure the change in the impedance of the magnetic beads as a function of PSA concentrations. When a BEIS sensor was characterized, its measurement was based on a three-electrode setup using an Autolab measurement system (Autolab® PGSTAT302N). For this configuration, an additional electrode was located outside of the

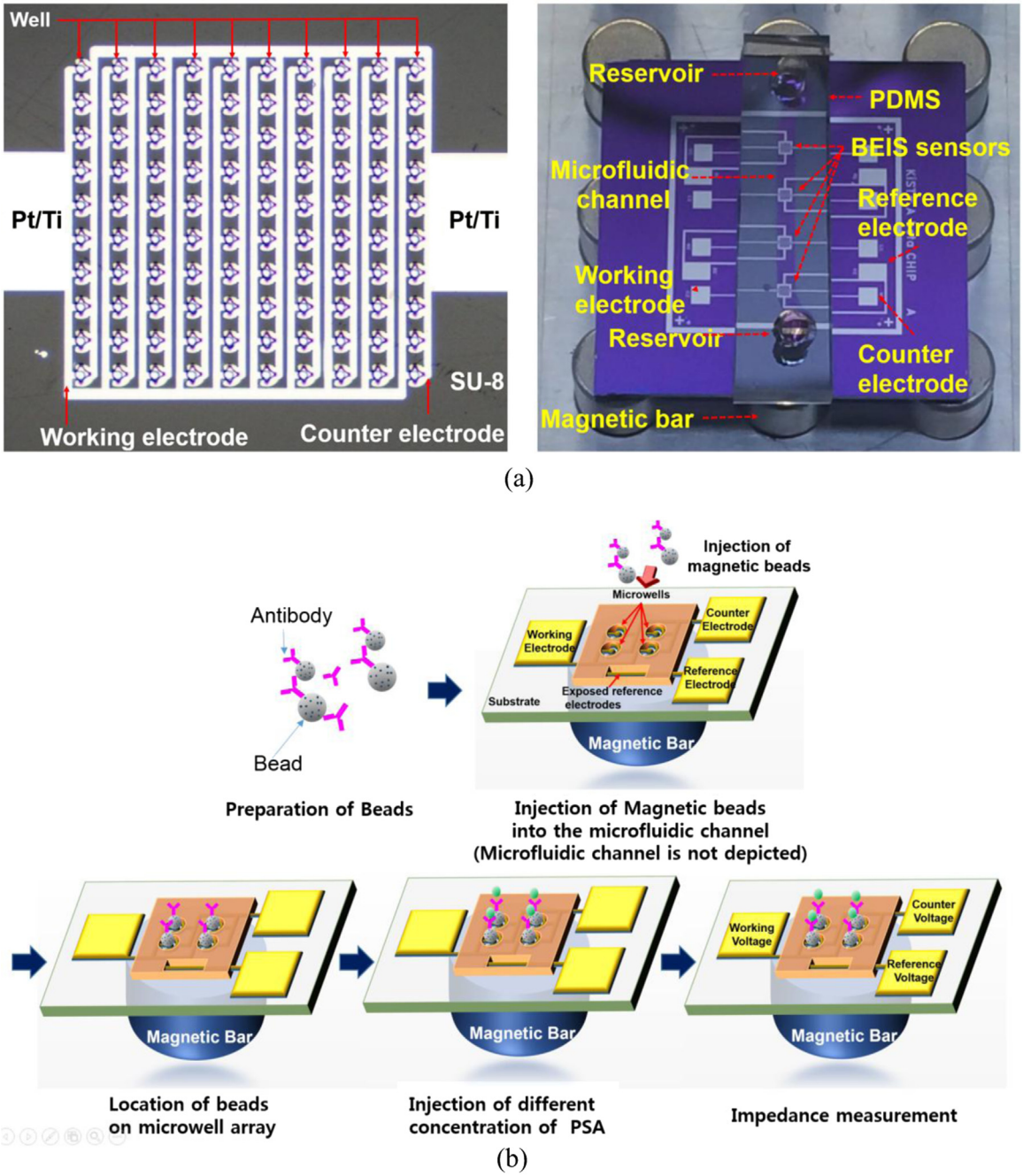

Fig. 1. Images of a proposed BEIS (Beads-based Electrochemical Impedance Spectroscopy) platform and experimental procedures; (a) images of the fabricated BEIS sensor and the BEIS platform with a magnetic bar, (b) Schematics of experimental procedures using BEIS platform,

BEIS sensor (reference electrode in Fig. 1(a)). During the frequency sweeping, the frequency was varied from 1 Hz to 1 MHz, while the amplitude of voltage was fixed at 50 mVrms.

3. Result and discussion

3.1. Operation principles based on electric field and equivalent electrical circuit

To investigate the effect of the microwell on the distribution of electric fields, a single well was modeled and simulated in COMSOL® software (Fig. 2) (Pryor, 2009). The simulation results confirmed that the distributions of electrical potential and electric field are strongly affected by a microwell. When a bead was positioned on the electrode (Fig. 2(a), left), the lines of electrical potential around/in a bead were more sparse than when a bead was near the edge of the electrode. If a bead was positioned near the edge of the electrodes, the distributions of electrical potential were almost similar around a bead regardless of a microwell (Fig. 2 (a), middle and right). However, it is difficult to locate a bead in a specific position without a guide structure such as the microwell. In addition, it was noted that the electrical potential distributions were weak above the SU-8 layer and that the most of the potential between the electrode and the buffer solution dropped within the SU-8 layer. A small decrease in the potential above the SU-8 layer generated very small leakage current. Electric fields were more concentrated around a bead than in the cases without a microwell

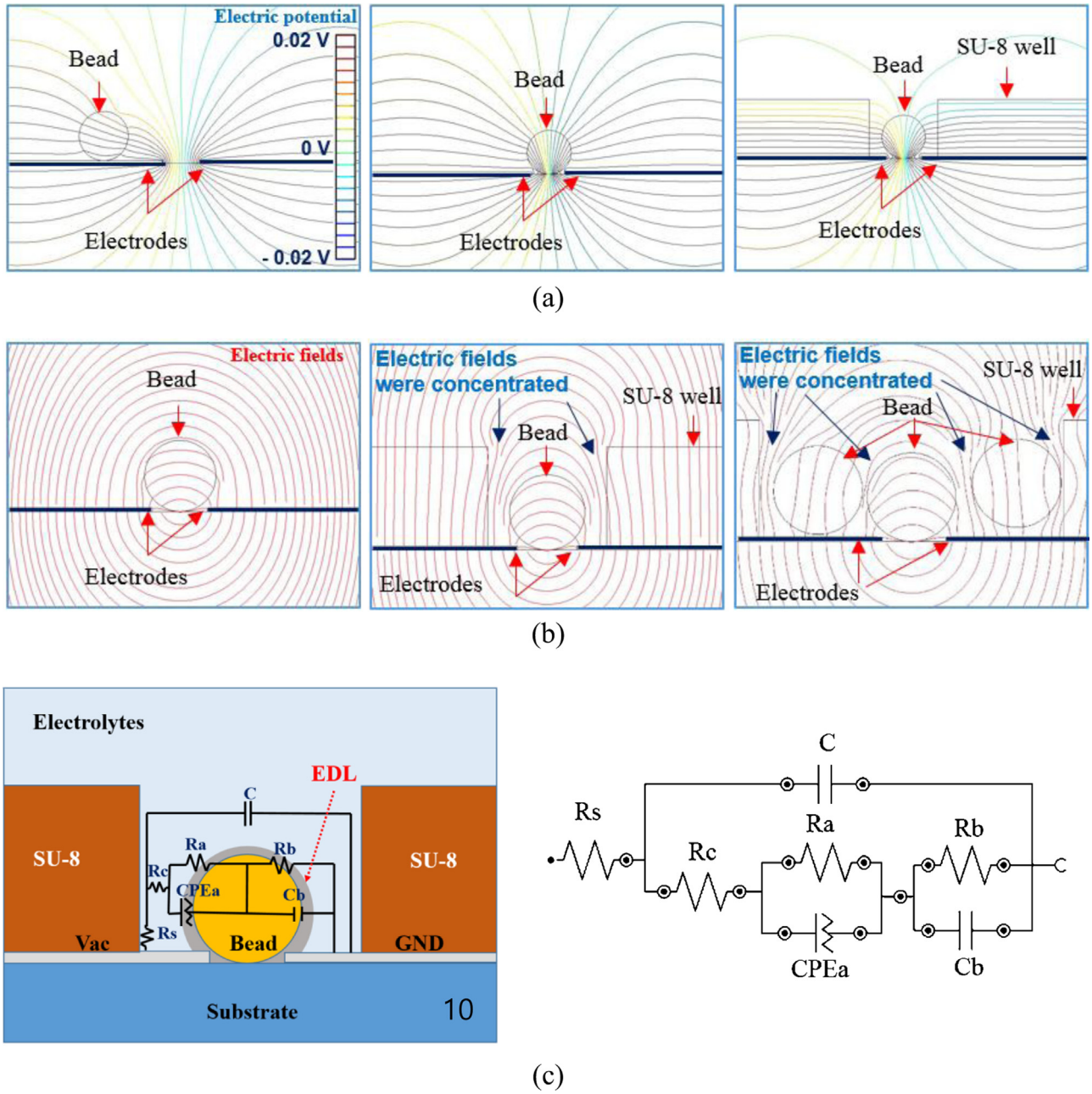

Fig. 2. Simulation results of the effect of a microwell on the distributions of electrical potential and elctric field from COMSOL software, *and equivalent electrical circuit for a BEIS platform*; (a) Distribution of electrical potential (left: a bead located on electrode without a microwell, middle: a bead located between electrodes without a microwell, a bead located between electrodes with a microwell), (b) Distribution of electric field (left: a bead located between electrodes without a microwell, middle: a bead located between electrodes with a microwell, right: three beads located between electrodes with a microwell), *(c) the structure of a BEIS sensor with consideration of electrical components (left) and the derived equivalent electrical circuit.*

(Fig. 2(b), left and middle). Although three beads were packed in a microwell, the electric fields effectively were confined around the magnetic beads (Fig. 2(b), right). Therefore, the structure of the microwell facilitated the location of a bead between the electrodes and also focused the electric fields on the beads (Fig. S2). The distribution of electrical potential is very important to understand the sensing mechanism of a BEIS sensor. As the lines of electrical potential around the beads becomes dense, the electric field strength around a bead was increased. Then, more ion charges in the buffer solution will cover the surface of a bead at lower frequency to form the electrical double layer (EDL). The electric fields are stronger in the bottom part of a bead, which means that a thicker EDL is generated there than in the other surface region. When charged biomolecules bind to the surface of a bead, they perturb the EDL, and the changes in the EDL layer resulting from the deformation of electrical field and ion diffusion result in a measurable changes in the impedance (Nagaraj et al., 2014). Therefore, the higher electric field forces more charges on the beads to form the EDL region, and they also push more biomolecules into the EDL region close to the surfaces of beads. In terms of net charge of the beads, the absorption or reaction of biomolecules modulates the net charges on the beads, and ion diffusion near the EDL region compensates for the change. Since the isoelectric point of PSA is between 6.8 and 7.5, PSA has negative charges in the PBS buffer (pH ~7.4). As the concentration of PSA antigen is increased, more PSA antigens are accumulated on the surfaces of the magnetic beads and more negative charges on the surfaces of magnetic beads in EDL region. Therefore, the increment of PSA

concentration results in decreasing the impedance of a BEIS sensor due to the ion diffusion caused by the perturbation of the EDL region. The changes in impedance that occurs *when* biomolecules are absorbed also can be explained by an electrical equivalent circuit. The BEIS sensor was modeled as an equivalent electrical circuit considering the structure of a sensor (Fig. 2(c)), which are composed of one constant-phase element, two capacitors, and four resistors. Rs is an electrolyte resistance, Rc is a contact resistance between the electrolyte and the EDL region, C is a capacitance between electrodes, and CPEa and Ra are a constant-phase element and a resistance between the electrolyte and the antigen in EDL region, respectively. Cb and Rb are a capacitance and a resistance between the antigen in EDL region and the beads, respectively. The changes in PSA concentration will induce changes in Rc, CPEa, Ra and Cb in the equivalent electrical circuit. Especially, Rc and CPEa are affected by the ion diffusion between the electrolytes and the antigen in EDL, Ra and Cb are related to the charge amount of the antigen on beads. The values of Rc, CPEa, Ra and Cb will show the different trends in increasing the concentration of PSA antigen. Rc and Ra are reduced by increasing ion diffusion and changes in the surface charge caused by PSA antigen. CPEa and Cb are increased by increasing the concentration and the

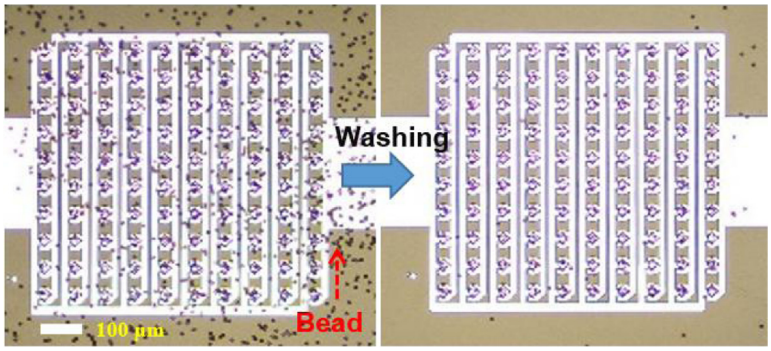

(a)

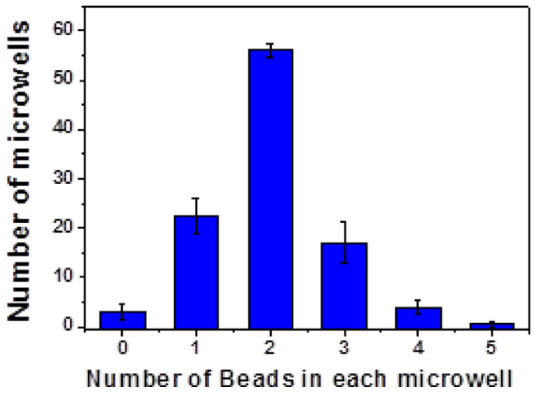

(b)

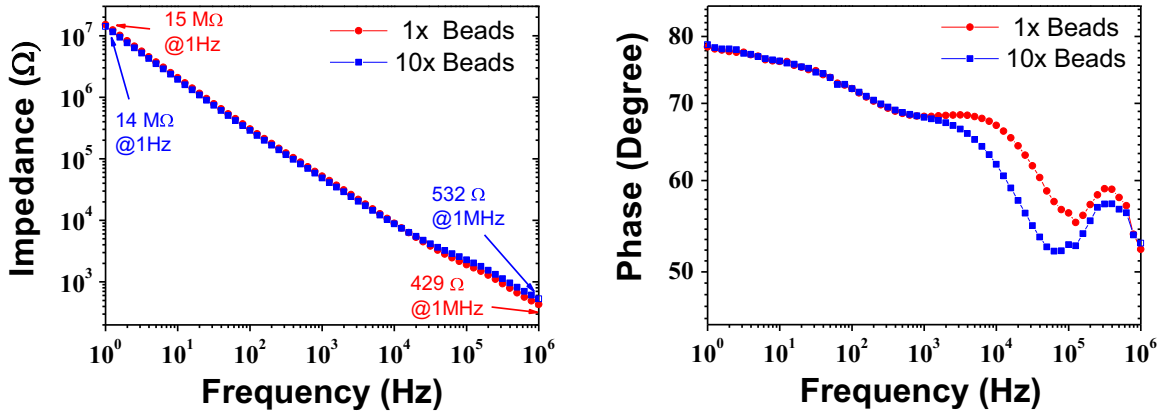

(c)

Fig. 3. The results of control experiments with magnetic beads in a BEIS platform; (a) the image of pre-treated beads after injection into the microfluidic channel (left) and the image of of pre-treated beads after the washing step, only a few beads were remained on the surface of SU-8 2005 (right), (b) distribution graph for the number of beads in the wells of a BEIS sensor (N=3, total number of microwells in a BEIS senosr is 100), (c) output responses from a BEIS platform when the concentration of beads was increased by a factor of 10 without a washing step; two different concentration of beads was injected into microfluidic channel to vary the number of beads *(3 ng/mL for 1x case, 30 ng/mL for 10x case).*

effective binding area of PSA antigen on the beads. Those changes cause a decrease in the total impedance of the equivalent circuit.

3.2. Control experiments with magnetic beads

Before conducting the whole process of PSA detection, first, we checked the distribution of beads in the microwell-array after the injection of the solution of magnetic beads. The number of beads tended to increase slightly when the injection time was longer or the flow rate is slower. The residue beads on the surface of SU-8 were washed away with slightly higher flow rate than that of the bead injection flow. The flow rates of 2 μl/min and 10 μl/min were used for the bead injection and washing steps, respectively. After the washing step, we could still observe some of beads remaining on the SU-8 passivation surface (Fig. 3(a)). However, those beads did not affect the impedance measurement of the captured beads, since the passivation layer blocked any effect of the uncaptured beads. The distribution of the number of beads followed the Poisson distribution, and it was difficult to find a microwell that had more than five beads in the experiments (Fig. 3(b)). In most cases, the number of beads trapped in a microwell ranged from one to three, and the microwells with two beads were dominant in every experiment. However, it is possible that the number of beads could have changed during the experimental procedures. We assumed the worst case as the number of beads was more than the normal case by a factor of 10 times, and we conducted an experiment to determine the effect of an abnormal number of beads on the output impedance and phase from a BEIS platform (Fig. 3(c)). In the worst-case experiment, the washing step was skipped to increase the number of beads around an array of wells. *In order to increase the number of beads, we used 10 times more concentrated magnetic beads, which is around 30 ng/mL. However, it does not mean that the number of beads in microwells are also increased by same factor but more beads can be easily stacked and distributed on/around microwells as the concentration of beads is increased.* The impedance plot shows that the change of impedance at lower frequency was smaller than that at higher frequency. The impedance changes are less than 7% at 1 Hz and around 19% at 1 MHz, respectively, while the phase was changed only in the range from 1 kHz to 1 MHz. Although the impedance was changed slightly in the lower frequency range in the worst case, it could be ignored in the normal experimental procedure because the washing step reduced the variation in the number of beads in the wells as depicted in Fig. 3(b).

3.3. Results of PSA detection with a BEIS platform

The concentration of PSA antigen was changed from 1 fg/mL to 10 ng/mL in the PBS buffer. Fig. 4 shows the Nyquist, impedance and phase results with varying concentrations of PSA antigen as a function of frequency. It is clear that the changes in the concentration of PSA antigen can effectively modulate the output responses from a BEIS platform due to the changes in the charge on the beads caused by PSA antigen. Note that the impedance changes were dominant at lower frequencies, and the phase changes were in a medium frequency range (1–100 kHz). However, the number of beads and the ion concentration of PBS buffer also affects the phase values in the medium frequency range. Therefore, it is difficult to separate the effect of PSA antigen on the phase plot from the mixed signal combined with the number of beads and the ion concentration of the buffer solution. Fortunately, the number of beads did not affect the impedance significantly at lower frequencies if the buffer solution was not changed during the experimental procedure. Therefore, it is recommended that a low frequency impedance be chosen to determine the concentration of PSA antigen using a pre-defined buffer solution. The

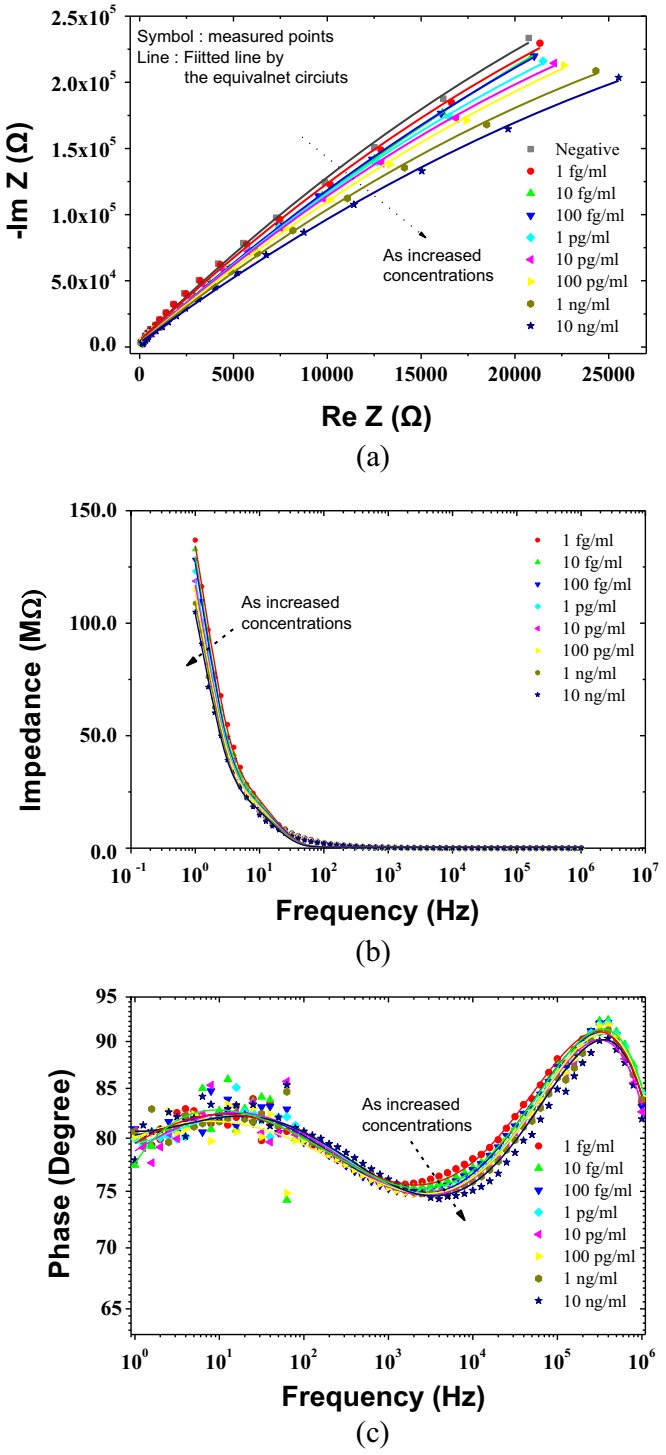

Fig. 4. Output responses from a BEIS platform according to various concentrations of PSA antigen; (a) Nyquist responses with varying concentration of PSA antigen, (b) impedance responses as a function of frequency, (c) phase responses as a function of frequency.

responses measured and the results extracted from the equivalent circuit (Fig. 2(c)) are exhibited as symbols and lines, respectively in Fig. 4. The extraction was conducted in three steps with the equivalent electrical circuit. First, four parameters of Ra, CPEa, and Cb were initially fitted by NOVA® software using the measured responses as a function of the concentration of PSA antigen *with the assumption that other three parameters of Rs, C and Rb are constant to find the dominant parameter.* Secondly, each parameter of Rc, Ra, CPEa, and Cb was arranged with varying concentrations

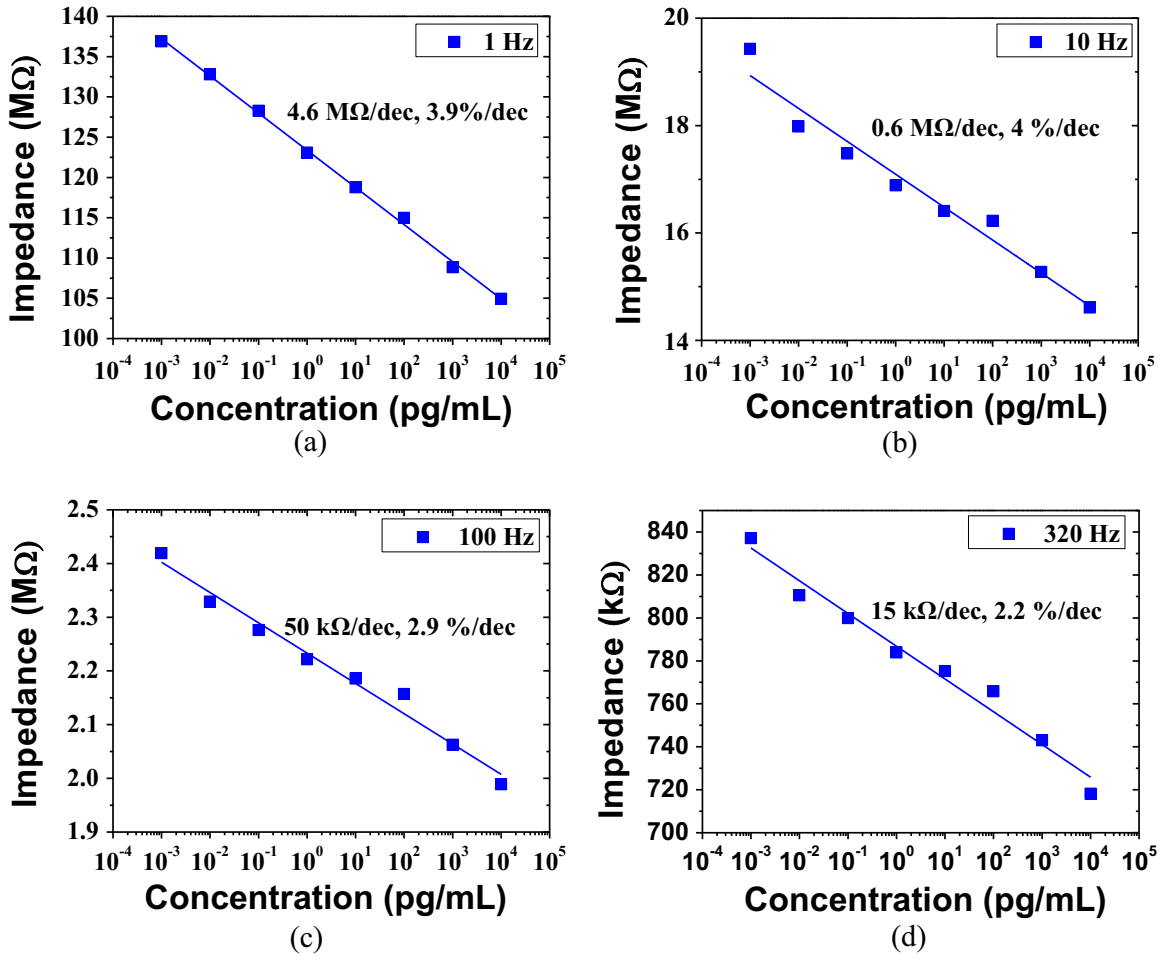

Fig. 5. Dependance of applied frequency on the sensitivity as a function of concentraion of PSA antigen; (a) sensitivity is approximately 4.6 MΩ/dec at 1 Hz, (b) sensitivity is approximately 0.6 MΩ/dec at 10 Hz, (c) sensitivity is approximately 50 kΩ/dec at 100 Hz, (d) sensitivity is approximately 15 kΩ/dec at 320 Hz.

of PSA, and its linear relationship is extracted by linear fitting for each parameter (as shown in Fig. S3). Third, all lines of Fig. 4 at the different concentration were collected by applying all refined values of Rc, Ra, CPEa, Cb to the equivalent circuit in the simulation mode in NOVA software, where refined values are deducted from the fitted lines at specific concentrations in Fig. S3. All of the lines that were extracted coincided well with the symbolic responses with chi-squared in the range of 0.045–0.061. *Although, the chi-squared values are slightly larger than 0.05, these results imply that it is acceptable that Rc, Ra, CPEa, and Cb are the dominant factors rather than Rs, C and Rb in the equivalent electrical circuit.*

3.4. Sensitivity and limit of detection of a BEIS platform for PSA detection

In order to evaluate the frequency effect on outputs responses as a function of PSA antigen, the outputs of impedance were plotted in Fig. 5 at different specific frequencies. The slope and the linearity of the lines are important, since each slope represents the sensitivity of a BEIS sensor at specific frequency. The slopes of impedance decreased exponentially, from 4.6 MΩ/dec to 15 kΩ/dec, with the increment of measuring frequency. However, it is not a good way to define the sensitivity as the slope of absolute impedance, since devices have some variations in the sensitivities caused by different impedance levels, even though they were fabricated at the same time or in the same batch. To resolve the variation of sensitivity due to differences from device to device, we defined a normalized sensitivity as the ratio of impedance changes at a concentration of PSA antigen normalized by the initial reference impedance as:

$$\text{Normalized Sensitivity}(\%/\text{dec}) \sim \left| \frac{Z_{PSA} - Z_{Buffer}}{Z_{Buffer}} \right| \times 100 \quad (1)$$

where, Z_{PSA} and Z_{Buffer} are the impedances at a concentration of PSA antigen in buffer solution and the impedance in only buffer solution, respectively.

Therefore, when the sensitivities are expressed as normalized sensitivities, their differences are of the same order. They are almost constant at frequencies less than 10 Hz, and they began to decrease slightly above 10 Hz. The linearity was the best at 1 Hz for which the linear recession value was 0.998, and it was degraded to 0.971 with the increment of frequency. Therefore, it was concluded that the sensitivity and the linearity are enhanced by decreasing the frequency of applied voltage.

We tested multiple devices (N=4) in a platform to evaluate the LOD of detecting PSA in PBS using average slope. Fig. 6(a) shows the average impedance as a function of the concentration of PSA at 1 Hz, and the sensitivity was approximately 5.3 MΩ/dec. The normalized impedance converted by Eq. (1) (Fig. 6(b)) gives the normalized sensitivity in percentage as approximately 3.6%/dec. The error bar at 1 fg/mL of PSA antigen is so large that some of the sensors could not distinguish the signal change of PBS buffer with those at 1 fg/mL of PSA antigen. Above 10 fg/mL of PSA antigen, the error bars were small enough to discriminate the value of the next point. Hence, it is reasonable to define the LOD of a BEIS platform

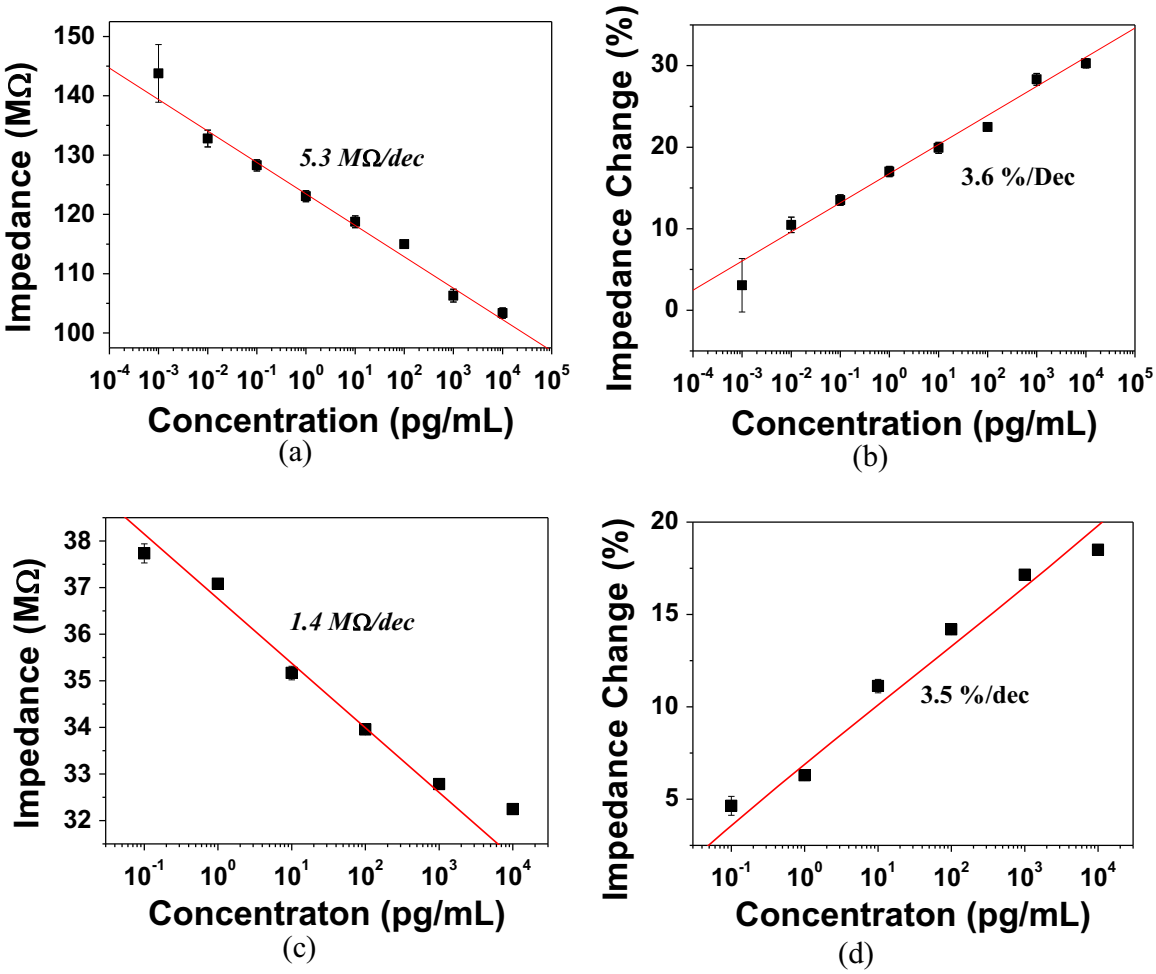

Fig. 6. Sensitivities of BEIS platforms for detection of PSA antigen in PBS buffer and in human plasma; (a) sensitivity is 5.3 MΩ/dec at 1 Hz in PBS buffer, (b) sensitivity in percentage is 3.6%/dec at 1 Hz in PBS buffer, (c) sensitivity is 1.4 MΩ/dec at 1 Hz in human plasma, (d) sensitivity in percentage is 3.5%/dec at 1 Hz in human plasma.

as above 10 fg/mL. The LOD is comparable to that of a nanotechnology-based biosensor (Kim et al., 2007).

Next, human plasma was spiked with the known concentrations of PSA in the range of 100 fg/mL and 10 ng/mL. To determine the initial reference impedance (Z_{Buffer}) of human plasma in a BEIS platform, human plasma was injected into a microfluidic channel for 5 min and washed by 0.1x PBS buffer, and the impedance was used as an initial reference. All impedance levels with varying concentrations of PSA in plasma were measured and plotted, as shown in Fig. 6(c) and (d). The impedance levels and slope of impedance were different from those of the previous PSA experiment in PBS buffer due to the changes in the fabricated devices (Fig. 6(c)). However, the normalized sensitivity in percentage was 3.5%/dec, which was close to that of PSA in PBS (3.6%/dec). Hence, the normalized sensitivity was useful to compensate for the variations in the impedances of the devices. The linearities in Fig. 6 (b) and (d) were about the same in the PBS buffer and human plasma, i.e., 0.983 and 0.981, respectively. The LOD of PSA in human plasma was estimated as approximately 100 fg/mL, which was higher than the previous LOD of PSA in PBS by a factor of 10, but it is still comparable to that of the best EIS sensors or the nanotechnology-based biosensor. *In addition, we checked the reusability of a BEIS platform to detect the PSA antigen and confirmed that the sensor can be 3–5 times reusable. The testing results for reusability (N=3) were depicted in Fig. S4 in the supplementary.*

4. Conclusion

A particle-based reusable electrochemical immunosensor using magnetic beads demonstrated its advantage of repeated use, but its detection limit (> 100 pg/mL) were greater than those of recently-reported EIS sensors. Hence, there are difficulties in applying BEIS to an early diagnosis of a disease due to its relatively low sensitivity. We proposed a novel BEIS platform with a microwell array to push the LOD of reusable EIS devices to sub pg/mL levels by sustaining the recyclability of the BEIS sensor. Microwell arrays were used to concentrate the electric field on the surfaces of magnetic beads to improve the sensitivity.

The performance of the BEIS platform with a microwell array was confirmed by the immunoassay of prostate specific antigen (PSA). The experimental results showed that the BEIS platform with a microwell array could detect PSA with much higher sensitivity at low frequency. It could detect levels of a few tens of fg/mL in the PBS buffer and levels of a few hundreds of fg/mL of PSA antigen in the human plasma. The LODs of the proposed BEIS platform are comparable to those of advanced biosensors based on nanotechnology, but BEIS has the advantageous of having a simple fabrication process, low cost, and reusability. Since we demonstrated that the BEIS platform with a microwell array is a highly sensitive and rugged non-labeled biosensor platform, it is expected to one of the valuable platforms in immunoassays that require high sensitivity.

Acknowledgments

This research was supported mainly by the Open Research Program through the Internal Fund of the Korea Institute of Science and Technology (2E25740, 2E25590). It was also supported by the Bio & Medical Technology Development Program of the NRF funded by the Korean government, MSIP (NRF-2015M3A9E2028888), the Industry Core Technology Development Project of KEIT funded by the Korean Government, MOTIE (KEIT-10060305) and a grant of the Korea Health Technology R&D Project through the Korea Health Industry Development Institute (KHIDI), funded by the Ministry of Health & Welfare, Republic of Korea (HI14C3319).

Appendix A. Supplementary material

Supplementary data associated with this article can be found in the online version at http://dx.doi.org/10.1016/j.bios.2016.04.086.

References

Akter, R., Kyun Rhee, C., Aminur Rahman, M., 2014. Biosens. Bioelectron. 54 (0), 351–357.
Association, A.U., 2000. Oncology 14, 261–267.
Brazhnik, K., Sokolova, Z., Baryshnikova, M., Bilan, R., Efimov, A., Nabiev, I., Sukhanova, A., 2015. Nanomed. Nanotechnol. Biol. Med. 11 (5), 1065–1075.
Centi, S., Tombelli, S., Minunni, M., Mascini, M., 2007. Anal. Chem. 79 (4), 1466–1473.
Chiriaco, M.S., Primiceri, E., Montanaro, A., de Feo, F., Leone, L., Rinaldi, R., Maruccio, G., 2013. Analyst 138 (18), 5404–5410.
Choi, J.H., Kim, H.S., Choi, J.-W., Hong, J.W., Kim, Y.-K., Oh, B.-K., 2013. Biosens. Bioelectron. 49 (0), 415–419.
Chuah, K., Lai, L.M.H., Goon, I.Y., Parker, S.G., Amal, R., Justin Gooding, J., 2012. Chem. Commun. 48 (29), 3503–3505.
Ewers, M., Sperling, R.A., Klunk, W.E., Weiner, M.W., Hampel, H., 2011. Trends Neurosci. 34 (8), 430–442.
Gao, A., Lu, N., Dai, P., Fan, C., Wang, Y., Li, T., 2014. Nanoscale 6 (21), 13036–13042.
Gao, A., Lu, N., Wang, Y., Dai, P., Li, T., Gao, X., Wang, Y., Fan, C., 2012. Nano Lett. 12 (10), 5262–5268.
Haes, A.J., Chang, L., Klein, W.L., Van Duyne, R.P., 2005. J. Am. Chem. Soc. 127 (7), 2264–2271.
Hu, Y., Zuo, P., Ye, B.-C., 2013. Biosens. Bioelectron. 43 (0), 79–83.
Huang, Y.-W., Wu, C.-S., Chuang, C.-K., Pang, S.-T., Pan, T.-M., Yang, Y.-S., Ko, F.-H., 2013. Anal. Chem. 85 (16), 7912–7918.
Jang, H.D., Kim, S.K., Chang, H., Choi, J.-W., 2015. Biosens. Bioelectron. 63, 546–551.
Jia-dong, L., Jun-jie, C., Bin, M., Xiao-wei, W., Jie, X., Jin-cheng, Z., Zhi-qiang, Z., Dong-min, W., 2014. J. Micromech. Microeng. 24 (7), 075023.
Johnson, E.D., Kotowski, T.M., 1993. J. Forensic Sci. 38 (2), 250–258.
Kim, A., Ah, C.S., Yu, H.Y., Yang, J.-H., Baek, I.-B., Ahn, C.-G., Park, C.W., Jun, M.S., Lee, S., 2007. Appl. Phys. Lett. 91 (10), 103901.
Lee, J.H., Hwang, K.S., Park, J., Yoon, K.H., Yoon, D.S., Kim, T.S., 2005. Biosens. Bioelectron. 20 (10), 2157–2162.
Lee, J.U., Nguyen, A.H., Sim, Sang J.,, 2015. Biosens. Bioelectron. 74 (0), 341–346.
Li, C., Curreli, M., Lin, H., Lei, B., Ishikawa, F.N., Datar, R., Cote, R.J., Thompson, M.E., Zhou, C., 2005. J. Am. Chem. Soc. 127 (36), 12484–12485.
Liu, G., Lin, Y., 2005. J. Nanosci. Nanotechnol. 5 (7), 1060–1065.
Luo, X., Davis, J.J., 2013. Chem. Soc. Rev. 42 (13), 5944–5962.
Mao, K., Wu, D., Li, Y., Ma, H., Ni, Z., Yu, H., Luo, C., Wei, Q., Du, B., 2012. Anal. Biochem. 422 (1), 22–27.
Mohd Azmi, M.A., Tehrani, Z., Lewis, R.P., Walker, K.A.D., Jones, D.R., Daniels, D.R., Doak, S.H., Guy, O.J., 2014. Biosens. Bioelectron. 52 (0), 216–224.
Nagaraj, V.J., Jacobs, M., Vattipalli, K.M., Annam, V.P., Prasad, S., 2014. Env. Sci. Process. Impact 16 (1), 135–140.
Oh, J., Yoo, G., Chang, Y.W., Kim, H.J., Jose, J., Kim, E., Pyun, J.-C., Yoo, K.-H., 2013. Biosens. Bioelectron. 50 (0), 345–350.
Pryor, R.W., 2009. Multiphysics Modeling Using COMSOL: A First Principles Approach. Jones & Bartlett Publishers.
Rusling, J.F., 2013. Anal. Chem. 85 (11), 5304–5310.
Sarkar, P., Ghosh, D., Bhattacharyay, D., Setford, S.J., Turner, A.P.F., 2008. Electroanalysis 20 (13), 1414–1420.
Shariat, S.F., Semjonow, A., Lilja, H., Savage, C., Vickers, A.J., Bjartell, A., 2011. Acta Oncol. 50 (S1), 61–75.
Wen, X., Gupta, S., Wang, Y., Nicholson, T.R., Lee, S.C., Lu, W., 2011. Appl. Phys. Lett. 99 (4), 043701.
Wu, G., Datar, R.H., Hansen, K.M., Thundat, T., Cote, R.J., Majumdar, A., 2001. Nat. Biotech. 19 (9), 856–860.
Yang, J., Wen, W., Zhang, X., Wang, S., 2015. Microchim Acta 182, 1855–1861.
Zhang, Y., Yan, Y., Chen, W., Cheng, W., Li, S., Ding, X., Li, D., Wang, H., Ju, H., Ding, S., 2015. Biosens. Bioelectron. 68 (0), 343–349.